The role of hesperidin in ameliorating retinal changes in rats with experimentally induced type 1 diabetes mellitus and the active role of vascular endothelial growth factor and glial fibrillary acidic protein

Azza Saad Shehata[1], Dalia Abduelmoein Mohamed[1], Sherein Mahmoud Hagras[3], Shimaa Mohsen El-Beah[4], Heba Mohamed Elnegris[1,2]

[1]Department of Histology and Cell Biology, Faculty of Medicine, Zagazig University, Zagazig, [2]Department of Histology and Cell Biology, Faculty of Medicine, Badr University in Cairo, Cairo, [3]Ophthalmology Center, Faculty of Medicine, Mansoura University, Mansoura, [4]Department of Biochemistry and Molecular Biology, Faculty of Medicine, Mansoura University, Mansoura, Egypt

Abstract: Patients with type 1 diabetes mellitus (T_1DM) are vulnerable to developing diabetic retinopathy even under insulin therapy. Thus, this study was designed to evaluate the efficacy of hesperidin and insulin in rats with T_1DM compared with insulin alone in improving diabetic retinal changes. Eighty rats were divided into four equal groups: group I, control rats without diabetes; group II, untreated rats with diabetes; group III, rats with diabetes treated daily with subcutaneous (SC) doses of long-acting insulin; and group IV, a rat with diabetes in which hesperidin was orally administered with SC insulin. The animals were assessed histologically, morphometrically, and biochemically. In group II, the thickness of all retinal layers decreased histologically. Ultrastructurally, degenerated retinal neurons and congested blood vessels were observed. Immunostaining detected elevated gene expression of advanced glycation end products. Gene expression of vascular endothelial growth factor, and glial fibrillary acidic protein were elevated. In this study, hesperidin supplementation with insulin significantly improved the retinal histological changes, supported by morphometric findings, compared with insulin alone. Moreover, treatment with hesperidin significantly reduced malondialdehyde and elevated serum antioxidant markers, including superoxide dismutase and catalase; furthermore, glutathione peroxidase decreased. Hesperidin might be an effective supplement for improving diabetic retinal complications occurring even with insulin treatment.

Key words: Hesperidin, Retina, Type I diabetes mellitus, Vascular endothelial growth factor, Glial fibrillary acidic protein

Introduction

Many patients with diabetes may develop various complications along the course of the disease, including peripheral diabetic neuropathy, diabetic nephropathy, and diabetic retinopathy (DR). DR is a retinal microvascular disease that may eventually lead to loss of vision [1-3]. Some epidemiological studies have recognized several risk factors for DR, includ-

Corresponding author:
Heba Mohamed Elnegris (ORCID)
Department of Histology and Cell Biology, Faculty of Medicine, Zagazig University, Zagazig 44519, Egypt
E-mail: heba.negres@buc.edu.eg

ing long-standing diabetes, prolonged hyperglycemia, and hypertension. Genetic factors, body mass index, and dyslipidemia might also be risk factors for DR [4, 5].

Advanced glycation end products (AGEs) are the late products of nonenzymatic glycation, which are usually present in a substantially higher level in patients with diabetes. AGEs may promote retinal neuronal cell apoptotic loss. DR can be treated with intravitreal injection of vascular endothelial growth factor (VEGF) inhibitors, photocoagulation, or even pars plana vitrectomy. Nevertheless, these lines of treatment might not be able to preserve useful vision in advanced cases. Tight control of glucose levels is usually considered a corner stone in hindering the progression of DR [6]. Oral hypoglycemic agents and insulin remain the most popular drugs used in treating diabetes. However, hypoglycemia, weight gain, and drug resistance may complicate the use of these drugs. In contrast, several natural herbal medicines have demonstrated promising results in diabetic control with minimal adverse effects [7].

Formerly, there was much interest in natural hypoglycemic agents of plant origin as they were less toxic with few side effects. Ingestion of citrus fruits with their constituent flavonoids was proven to decrease the risk and increase survival in some chronic disorders [8]. A common component of our diet—bioflavonoids—has insulin-like properties and insulin receptor function [9].

Hesp (hesperetin 7-rhamnoglucoside) is a flavonoid that is obtainable from a group of species of citrus, including *Citrus aurantium* L. and Rutaceae *Citrus unshiu* [10]. Studies have reported that hesp has several biotic functions, such as antidiabetic, antihyperlipidemic, antioxidant, anticancer, antiatherogenic, and anti-inflammatory effects [11, 12].

This study was designed to assess the efficiency of hesp supplementation in improving histological, ultrastructural, and biochemical retinal impediments in albino rats with diabetes compared with that of insulin treatment alone and to elucidate the possible underlying mechanism.

Materials and Methods

Chemical and drugs

Streptozotocin (STZ) (catalog no. S0130) and hesp (catalog no. H5254) were obtained from Sigma Chemical Co. (St. Louis, MO, USA). Lantus (insulin glargine) was manufactured by Sanofi–Aventis (Frankfurt am Main, Germany). Glycation end product kits (1:200; catalog no. KAL-KH001)

were obtained from Cosmo Bio Co, Ltd. (Tokyo, Japan). All chemicals used in the biochemical analysis were purchased from Sigma Chemical Company.

Animals

Eighty 3-week-old male albino rats (body weight, 70±12 g) were incorporated into the experiment. They were placed in stainless-steel cages and kept at room temperature. The animals were fed on standard laboratory pellet diet and tap water *ad libitum* and were accommodated for 2 weeks before the start of the experiment. The experiment was conducted according to the Guide for the Care and Use of Laboratory Animals [13]. The local ethics committee of the Faculty of Medicine, Zagazig University, Egypt, approved this study (ID: 4476).

Animal grouping

The animals were randomly allocated into four equal groups (20 each) as follows:

Group I: this group was further divided into two subgroups:

Ia (control): The animals were injected intraperitoneally once with saline as a vehicle only.

Ib (positive control): The animals were received hesperidin by orogastric tube at a dose of 200 mg/kg [11].

The remaining 60 rats were treated with STZ to induce diabetes and were randomly divided into three equal groups:

Group II (type 1 diabetes mellitus [T_1DM]) consisted of rats with diabetes receiving no treatment.

Group III (insulin-treated diabetes) comprised rats with diabetes receiving daily subcutaneous (SC) injections of 2 units of long-acting insulin [14].

Group IV (insulin- and hesperidin-treated diabetes) consisted of rates receiving daily hesp at a dose of 200 mg/kg by orogastric tube along with a dose of insulin, similar to that in group III [15].

Induction of diabetes

In groups II, III, and IV, T_1DM was induced by a single intraperitoneal STZ injection after 12 hours of fasting at a dose of 50 mg/kg diluted in sodium citrate buffer (10 mM, pH 4.5) [16]. The rats were considered diabetic if the concentration of fasting tail blood glucose was higher than 200 mg/dl using a digital glucometer 2 days after the STZ injection [17]. Using a glucometer, blood samples from the tails were obtained weekly for measuring the blood glucose level along the study.

Sampling and histological analysis

The rats' health parameters were measured and recorded daily. The rats' weight was measured weekly until the end of the study. At the phase of sacrifice (8 weeks after diabetes confirmation), the animals were anesthetized with phenobarbital. Fasting blood specimens (after 12–14 hours) were taken from a tail vein and processed immediately into two tubes. The first tube contained fluoride for the immediate estimation of fasting blood glucose level, and the other tube was centrifuged after clotting at room temperature. The resulting sera were divided into small glass tubes and stored at −20°C before biochemical assessment. The right eye balls were finely dissected, and then, parts of the retina were snap-frozen in liquid nitrogen and stored at −80°C to measure the mRNA expression of glial fibrillary acidic protein (GFAP) and VEGF. For the light microscopy study, some left eye balls were prepared for routine histological examination and stained with H&E, following the method explained by Bancroft and Gamble [18]. For immunohistochemical study and recognition of AGEs, the sections were incubated using a labeled streptavidin–biotin kit (DAKO, Carpinteria, CA, USA) and were visualized using 3,3'-diaminobenzidine tetrahydrochloride [19, 20]. For the transmission electron microscopy study, small specimens of the retinae were prepared following the technique of Glauert and Lewis [21]. Ultrathin sections were examined using a JEOL-JEM 1010 electron microscope after being stained in the Department of Histology and Cell Biology, Faculty of Medicine, Zagazig University, Egypt.

Morphometric analysis

The thickness of different layers of the retina was measured in three planes of H&E-stained sections—central (100–150 μm away from the optic nerve), peripheral (100–150 μm away from the ora serrata), and mid peripheral sections (midway between the center and peripheral sections)—using "Leica Quin 500 C" image analyzer computer system (Leica Imaging System Ltd., Cambridge, UK). The measurements were recorded using a total magnification of ×400 [22]. The area of positive AGE immunostaining was measured in all retinal layers within 10 fields for each animal at a total magnification of ×400. Five sections obtained from five animals from the same group were used for measuring.

Biochemical analysis

Estimation of oxidant and antioxidant markers in retinal tissue

The left eyeball was prepared according to Saenz-de-Viteri et al. [23]. It was placed on a blotting paper, and an opening was made 5 mm posterior to the limbus to detach the anterior and posterior eye poles. Then, the retina was separated from the choroid complex using a scalpel blade and forceps. Once the retina samples were taken, they were positioned in plastic Eppendorf tubes with cold 0.9% saline phosphate-buffered saline (diluted ratio 1:5 according to their respective weight; pH 7.2). Using a mechanic homogenizer, the tissue was homogenized; then, the homogenate was centrifuged at 3,500 rpm for 15 minutes at 4°C. After centrifugation of

Table 1. Primer sequences and expected product size of genes amplified

Parameter	Reference sequence	Primer sequence	Fragment size (bp)
GAPDH	NM_017008.4	F: 5-TGCCACTCAGAAGACTGTGG-3	85
		R:5-GGATGCGGGATGATGTTCT-3	
GFAP	NM_017009.2	F:5-ACATCGAGATCGCCACCTAC-3	219
		R:5-ACATCACATCCTTGTGCTCC-3	
VEGF	NM_001110333.2	F: 5-CAATGATGAAGCCCTGGAGTG-3	219
		R: 5-GTCTGCGGATCTTGGACAAAC-3	

GAPDH, glyceraldehyde-3-phosphate dehydrogenase; GFAP, glial fibrillary acidic protein; VEGF, vascular endothelial growth factor.

Table 2. Data of body weight, serum glucose level, and area of AGE-positive immunoreactivity among the groups under study

Parameter	Control	T$_1$DM	T$_1$DM+insulin	T$_1$DM+insulin+hesp
Body weight (g)	215±2.1[d]	100 ± 2.5[a,b,c]	200±20.22[a,c,d]	220±10.33[b,d]
Food intake (g/day)	10.67±0.34[d]	15.12±0.2[a,b,c]	11.12±0.2[d]	11.43±0.22[d]
Serum glucose (mg/dl)	83.6±4.5[d]	350.62±65.5[a,b,c]	92.3±4.5[d]	84.6±8.2[d]
Area of AGE-positive immunostaining	0.030±0.62[b,d]	0.590±0.04[a,c]	0.511±0.03[a,c]	0.401±0.12[b,d]

Values are presented as mean±SD. T$_1$DM, type 1 diabetes mellitus; hesp, hesperetin 7-rhamnoglucoside; AGE, advanced glycation end products. [a]Significantly different from group I (P<0.05); [b]Significantly different from group III (P<0.05); [c]Significantly different from group IV (P<0.05); [d]Significantly different from group II (P<0.05).

the homogenate, the supernatant was collected and recentrifuged under the same conditions. The second supernatant was used for enzyme measurements. The oxidative stress status in the retinal homogenate was assessed by determining malondialdehyde (MDA), superoxide dismutase (SOD), glutathione peroxidase (GSH-Px), and catalase (CAT) using commercially available colorimetric kits (Biodiagnostic, Giza, Egypt) according to the manufacturer's instructions.

Quantitative estimation of plasma glucose levels
Plasma glucose was assessed using specific colorimetric glucose kit (Bioscience, Cairo, Egypt).

RNA extraction and quantitative real-time polymerase chain reaction (PCR)
For estimating VEGF and GFAP, the gene expression of GFAP and VEGF in retinal tissue was measured using real-time quantitative PCR (qPCR). Total RNA was isolated from frozen retinal tissues using RNeasy Mini Kits (Qiagen catalog no. 74104; Qiagen, Gemantown, MD, USA) according to the manufacturer's instructions. RNA concentration and purity in each sample were determined using the NanoDrop 2000c Spectrophotometer (Thermo Fisher Scientific, Rockford, IL, USA) using 260- and 260/280-nm ratios, respectively. Reverse transcription PCR was performed on 1 μg of total RNA using a QuantiTect® Reverse Transcription kit (Qiagen). The cDNA product was subjected to real-time PCR for the genes under study using SYBR green PCR master mix (Applied Biosystem SYBR® Green PCR Master Mix 2×, catalog no. 4344463; Life technology, Carlsbad, CA, USA) and primers specific for each gene. The primer sequences for glyceraldehyde 3-phosphate dehydrogenase (GAPDH), GFAP, and VEGF (Table 1). GAPDH was used as the reference gene. Primer sets were purchased from Vivantis Co. (Selangor Darul Ehsan, Malaysia). The real-time PCR program consisted of an initial step of enzyme activation at 95°C for 10 minutes, followed by 40 cycles of template denaturation at 95°C for 15 seconds, annealing at 60°C for 1 minute, and extension at 72°C for 45 seconds. Real-time PCR assays were performed on the Applied Biosystems 7500 real-time PCR detection system (Life technology). The specified gene transcription level was calculated using the comparative threshold method ($2^{-\Delta\Delta Ct}$) according to Livak and Schmittgen [24]. Melting curve analyses were used to verify the specificity of the PCR products.

Statistical analysis
Statistical data analyses were performed using Statistical Package for the Social Sciences (version 17; SPSS Inc., Chicago, IL, USA). The results of multiple groups were compared using one-way analysis of variance, followed by a post hoc test (least significant different test). The P-values of less than or equal to 0.05 were used to denote statistical significance.

Results

Body weight and general conditions
At the end of the study, group II had significantly decreased body weights and showed sluggishness, polyphagia, and polyuria. Fungal skin lesions were found in nine rats in group II, which were treated with topical treatment. Groups III and IV showed improvement in general health conditions. The mean body weight of group IV was significantly higher than that in groups II and III (Table 2).

Histological results

H&E-stained sections
Comparable histological results were obtained in both control groups (Ia and Ib); thus, group Ia was chosen as the control group in the analysis of the results. The histological structure of retinal layers of the control group consisted of photoreceptor outer segment (POS), outer nuclear layers (ONL), outer plexiform layers (OPL), inner nuclear layers (INL), inner plexiform layers (IPL), and ganglion cell layers (GCL) (Fig. 1A, E).

Group II (T_1DM) expressed an observable reduction in the thickness of all retinal layers. The ONL displayed fewer nuclei, most of which were dark. Furthermore, the nuclei of INLs were few and darker than those of the control and widely separated. The IPL showed widening of the spaces between nerve fibers. The GCL showed few cells with small nuclei. Some congested retinal blood vessels were observed (Fig. 1B, F). Similar retinal changes were noticed in group III (Fig. 1C, G). Group IV showed retinal layers with restored normal histological structure and thickness compared with groups II and III (Fig. 1D, H).

Immunohistochemical localization of AGEs
Immunoreactivity in all retinal layers was negative in
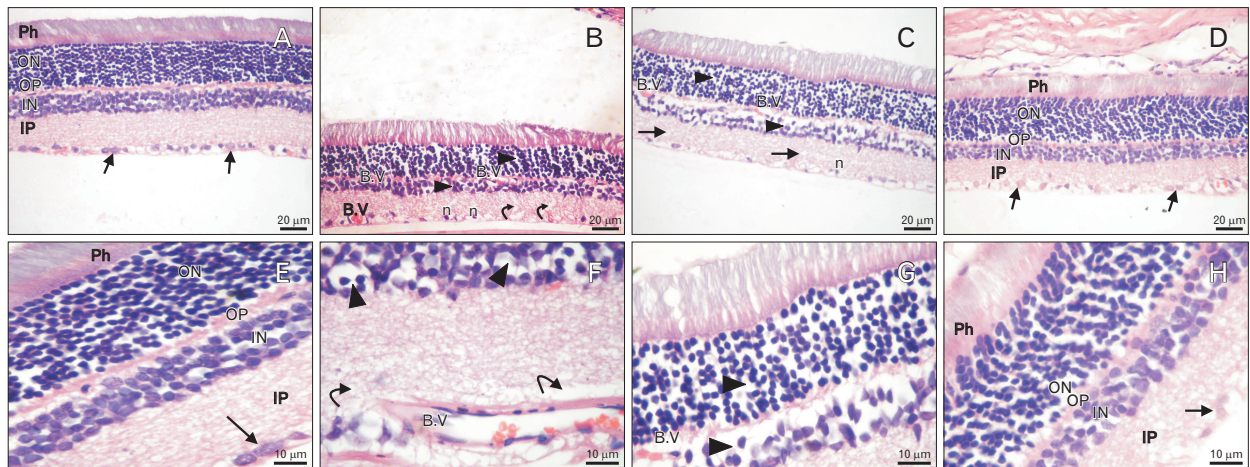
Fig. 1. Photomicrograph, paraffin sections stained with H&E, scale bar=20 μm (A–D: ×400), scale bar=10 μm (E–H: ×1,000). (A, E) Retina of control group: showing layers of the retina consisting of photoreceptor outer segment (Ph), outer nuclear (ON), outer plexiform (OP), inner nuclear (IN), inner plexiform (IP), and ganglion cell layers (arrow). (B, F) T$_1$DM group: showing observable decreased thickness of all retinal layers. Wide spaces appear between few and dark nuclei of outer and IN layers (arrow head). Nerve fibers of IP layer are widely separated (curved arrow). Ganglion cells are few with pyknotic nuclei (n). Congested B.V also seen. (C, G) Sections in retina of (T$_1$DM+insulin) group: showing decreased thickness of all retinal layers. Wide spaces appear between few and dark nuclei of outer and IN layers (arrow head). Nerve fibers of IP layer are widely separated (arrow). Ganglion cells are few and small n. Congested B.V also seen. (D, H) Retina of (T$_1$DM+insulin+hesp) group: showing layers of the retina with normal structure. Consisting of Ph, ON, OP, IN, IP, and ganglion cell layers (arrow). T$_1$DM, type 1 diabetes mellitus; hesp, hesperetin 7-rhamnoglucoside; B.V, blood vessel.
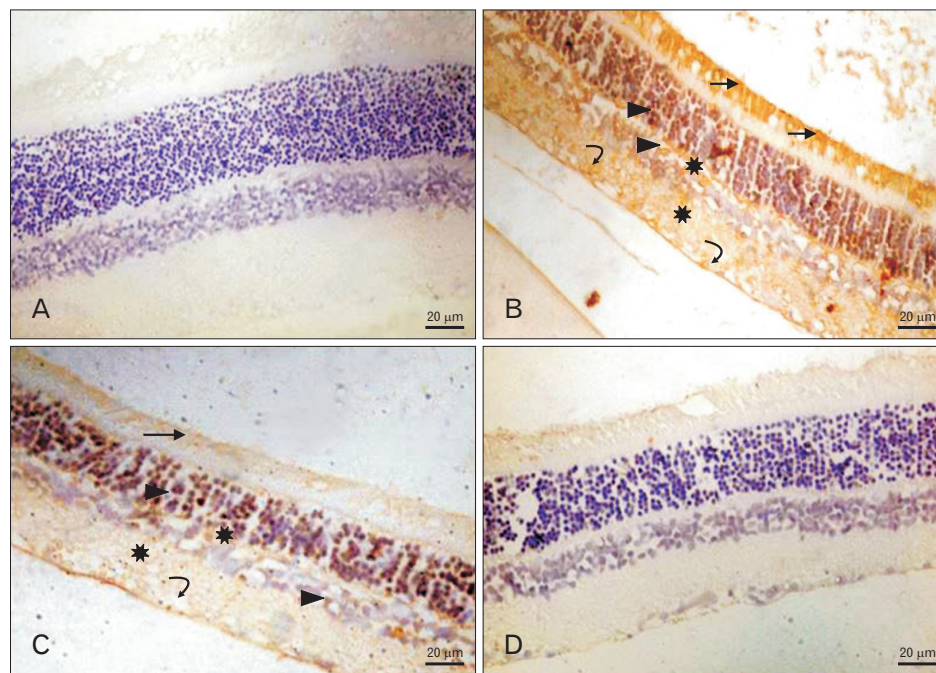
Fig. 2. (A–D) Photomicrograph, advanced glycation end products (AGE)-immunostained paraffin sections, scale bar=20 μm; Anti-AGE ×400. (A) Control group: showing negative cytoplasmic immunoreactivity in all retinal layers. (B) T$_1$DM group: showing strong positive cytoplasmic immunoreactivity in photoreceptor (black arrows), nuclear layers (arrowheads), plexiform layers (stars) and ganglion cell layer (curved arrows). (C) T$_1$DM+insulin group: showing mild positive cytoplasmic immunoreactivity in photoreceptor (arrow), nuclear layers (arrowhead), plexiform layers (stars) and ganglion cell layer (curved arrow). (D) T$_1$DM+insulin+hesp group: showing negative cytoplasmic immunoreactivity in all retinal layers. T$_1$DM, type 1 diabetes mellitus; hesp, hesperetin 7-rhamnoglucoside.

groups Ia and IV, strongly positive in group II, and mildly positive in group III in which immunoreactivity was noticed in the ONL and inner limiting membrane (Fig. 2).

Ultrastructural results

Electron microscopic examination of the control group revealed rod nuclei. They were small with highly condensed heterochromatin with a thin rim of cytoplasm around. The OPL appeared organized. The INL contained different neurons. The bipolar neurons showed large ovoid euchromatic nuclei with peripheral heterochromatin, few mitochondria, and few ribosomes. Müller cells showed oval electron-dense nuclei with abundant cytoplasmic processes. Amacrine cells were characterized by large indented nuclei. Retinal blood capillaries were noticed. The IPL seemed a thick layer of synaptic nerve fibers (Fig. 3).

Group II showed nuclei of rods widely separated and surrounded by vacuolated cytoplasm. The OPL appeared disorganized. Many neuronal alterations were found in the INL. Some neurons appeared degenerated with rarefied cytoplasm and dark nuclei. Other neurons seemed to have heterochromatic apoptotic nuclei. The cytoplasm of these cells contained irregular vacuoles. Neuronal nuclei with clumped chromatin were observed. Furthermore, dilated congested blood vessels with thick basement membrane were noted. Many Müller cells were electron dense with their processes
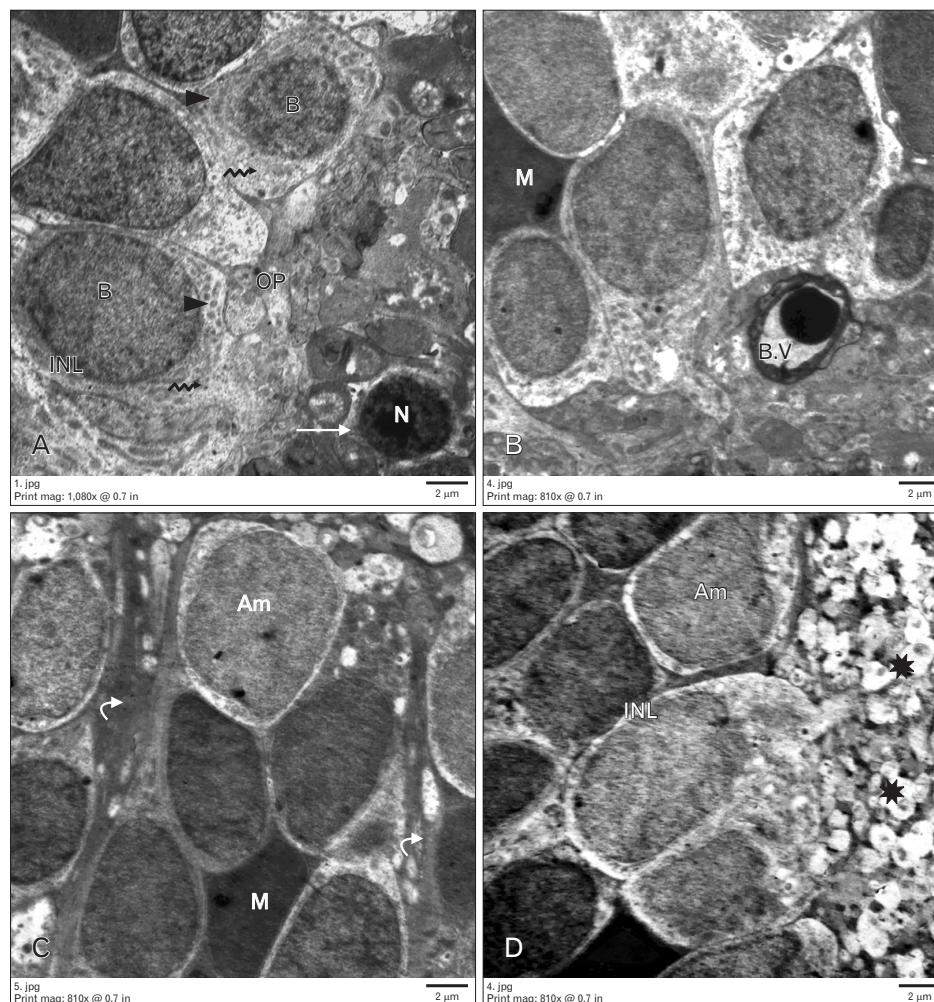
Fig. 3. Electron micrograph of control group, scale bar=2 μm (A: ×2,000; B–D: ×1,500). (A) Showing small highly condensed heterochromatic rod nuclei (N) with rim of cytoplasm (arrow), inner nuclear layer (INL) containing, bipolar neuron with large ovoid euchromatic nucleus (B), few mitochondria (arrowheads) and ribosomes (serrated arrows). Outer plexiform (OP) layer is seen. (B, C) Muller cells with oval electron dens nucleus (M) and cytoplasmic processes (curved arrow). Amacrine cell with indented nuclei is seen (Am), also retinal blood vessel (B.V) is seen. (D) Inner plexiform layer (stars) containing thick nerves fibers.
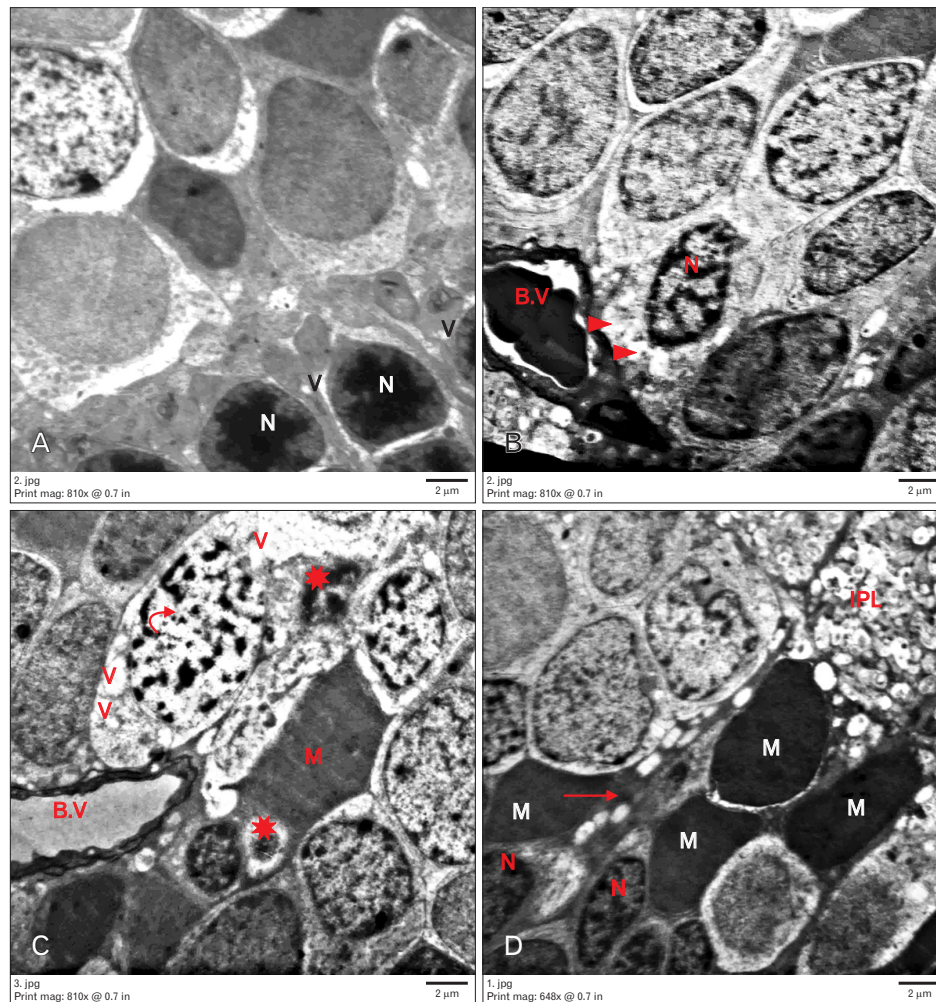
Fig. 4. Electron micrograph of type 1 diabetes mellitus (T₁DM) group, scale bar =2 μm (A–C: ×1,500; D: ×1,200). (A) Showing nuclei (N) of rods widely separated and surrounded with cytoplasm with multiple vacuoles (v). (B, C) Inner nuclear layer containing, degenerated neuron with rarified cytoplasm (arrowheads) and dark nuclei. Another neuron has apoptotic nucleus (star) and multiple cytoplasmic vacuoles (v), neuronal nuclei with clumped chromatin (curved arrow). Many Muller (M) cells also seen with its cytoplasmic processes (arrow), dilated congested retinal blood vessel (B.V) with thick basement membrane is present. (D) Microglia with dense nuclei are seen (N) and inner plexiform layer (IPL) are seen.

migrated in between INL. Microglia with dense nuclei and IPL were also observed (Fig. 4).

Group III showed rods with small electron-dense nuclei and a narrow OPL. Some neurons in the INL had rarefied vacuolated cytoplasm and nucleic remnants. Other cells appeared normal. Some blood vessels with normal diameter and intact basement membrane were observed. Furthermore, Müller cells were noted (Fig. 5).

Group IV revealed preserved ultrastructure of most retinal layers similar to that observed in the control group. The ONL contained electron-dense rod nuclei. The OPL appeared to have normal thickness and organization. Regard-ing the INL, many cells were found with electron-lucent cytoplasm and euchromatic nuclei, whereas others appeared to have heterochromatic nuclei. Furthermore, bipolar, ama-crine, Müller, and microglial cells were noted. Many blood vessels appeared to have a normal basement membrane (Fig. 6).

Morphometrical results

The differences in measurements between the two control subgroups were statistically insignificant. So, the records of group Ia were used as the control group in the statistical analysis. The thickness of all retinal layers was statistically decreased in groups II and III ($P<0.05$). A significant in-
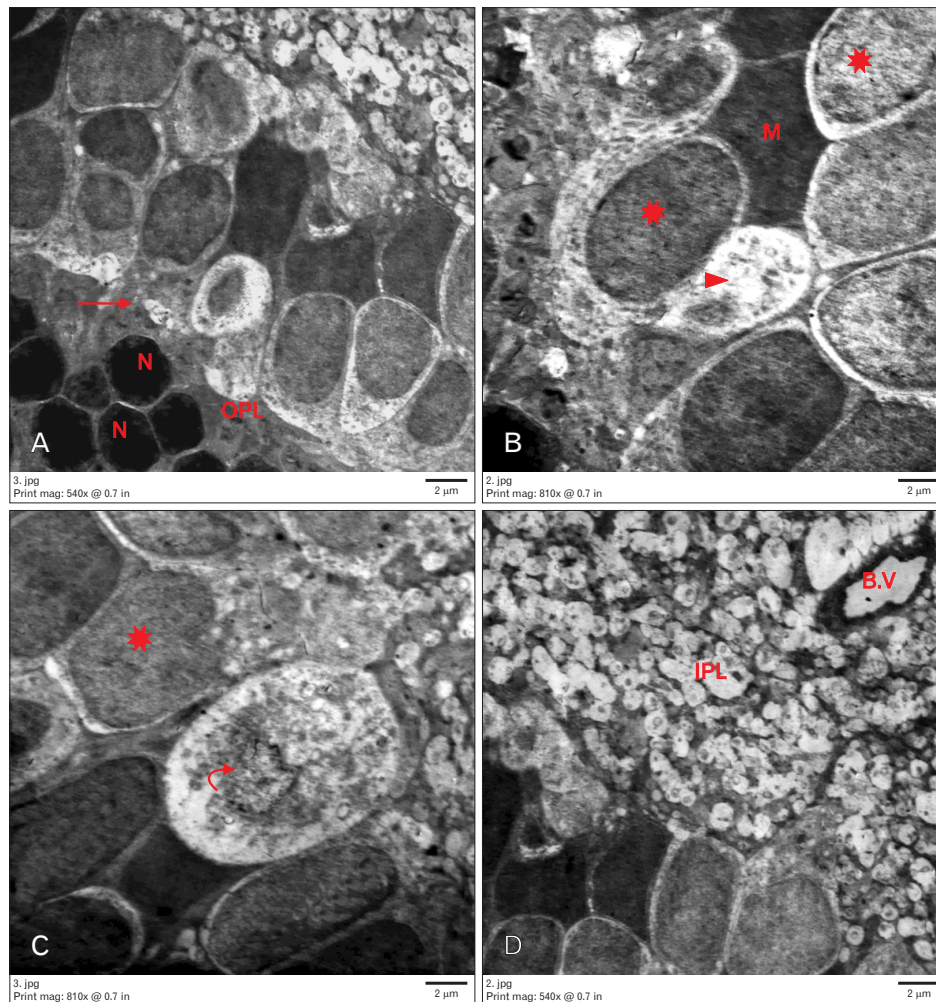
Fig. 5. Electron micrograph of (T$_1$DM+insulin) group, scale bar= 2 μm (A, D: ×1,000; B, C: ×1,500). (A) Showing rods with small electron dense nuclei (N) and narrow outer plexiform (OPL) (arrow). (B, C) Inner nuclear layer containing some neuron with rarified vacuolated cytoplasm (arrowhead) and remnants of nuclei (curved arrow). Another neuron appeared normal (stars). Muller cells (M) are also seen. (D) Retinal blood vessel with normal dimeter and intact basement membrane (B.V) and inner plexiform layer (IPL) are seen. T$_1$DM, type 1 diabetes mellitus.

crease in the thickness of the retinal layers was observed in group IV ($P<0.05$) without a statistically significant difference between groups IV and I (Fig. 7). The area of AGE-positive immunostaining in group II was statistically larger than that in group I ($P<0.05$). The area of AGE-positive immunostaining in group IV was statistically smaller than that in group II ($P<0.05$). The difference in the area of AGE-positive immunostaining between groups III and II was statistically insignificant (Table 2).

Biochemical results

Serum glucose and oxidative stress markers

The injection of STZ increased the mean serum glucose level to 350.62±65.5 mg/dl (Table 2) and reduced the mean serum insulin level as matched to the control group (data not shown). These levels returned to control values in groups III and IV (Table 2). A statistically significant decrease in the levels of antioxidant enzymes (*i.e.*, GSH-Px, SOD, and CAT) was observed in groups II and III compared with those in group I ($P<0.05$). However, a statistically significant increase in the levels of antioxidant enzymes was observed in group IV compared with those in group II ($P<0.05$). No significant
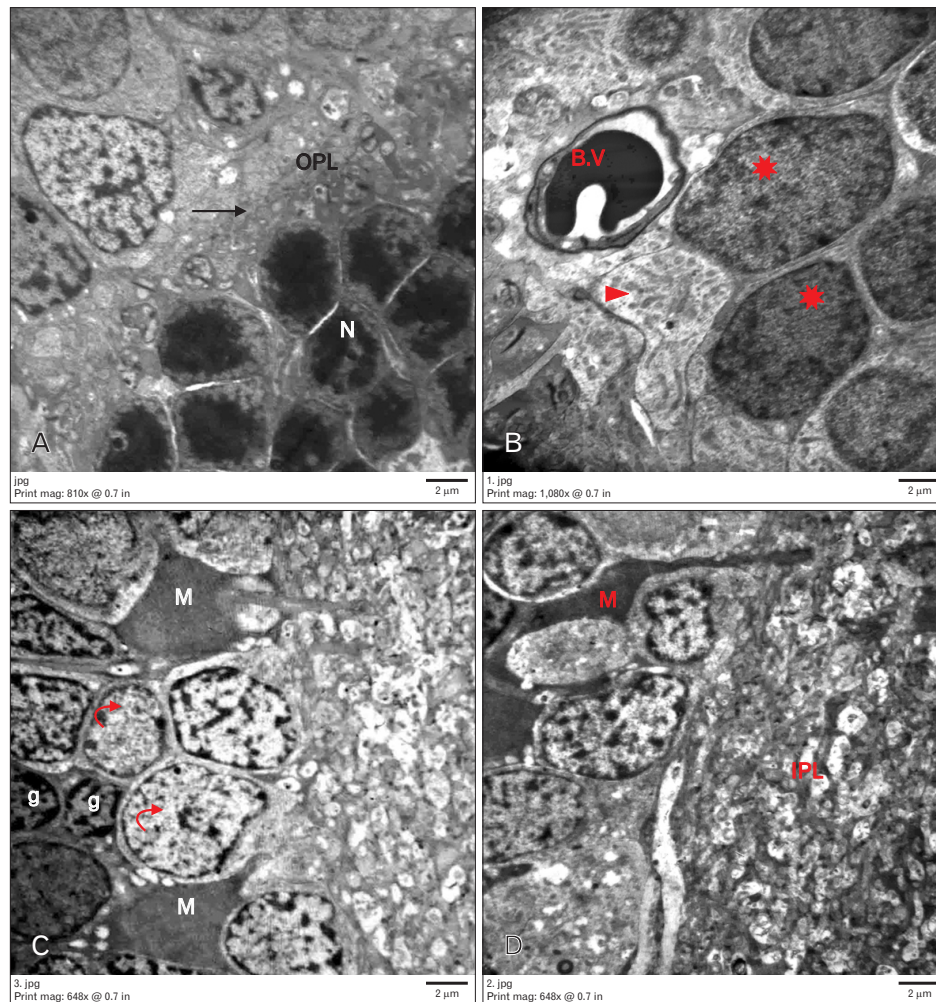
Fig. 6. Electron micrograph of (T$_1$DM+ insulin+hesp) group, scale bar=2 μm (A: ×1,500; B: ×2,000; C, D: ×1,200). (A) Showing preserved ultrastructure of most layers of retina. Rods with electron dense nuclei (N) and outer plexiform layer (OPL) with normal thickness an organization (arrow). (B–D) Inner nuclear layer containing many neurons with electron lucent cytoplasm (arrowheads) and euchromatic nuclei (curved arrows). Other neurons appeared with heterochromatic nuclei (star). Microglia (g), retinal blood vessel with normal basement membrane (B.V), Muller cells and inner plexiform layer (IPL) are seen. T$_1$DM, type 1 diabetes mellitus; hesp, hesperetin 7-rhamnoglucoside.

difference in antioxidant levels was observed between groups II and III. MDA significantly increased in groups II and III compared with that in the control group ($P<0.05$). However, a significant reduction in MDA level was observed in group IV compared with that in group II ($P<0.05$). No significant difference in MDA level was observed between groups II and III (Fig. 8).

GFAP gene expression levels in rat retina

Retinal gene expression of GFAP was significantly increased in groups II and III compared with that in group I ($P≤0.001$). GFAP expression in group IV decreased to values similar to those in the control group I. However, insulin could not return GFAP expression to normal levels (Fig. 9).

VEGF gene expression levels in rat retina

Retinal gene expression of VEGF was significantly increased in groups II and III compared with that in group I ($P≤0.001$). Furthermore, a significant increase in *VEGF* gene expression was observed in group III compared with that in group IV ($P≤0.001$). *VEGF* gene expression in group IV decreased to a level similar to that in group I (Fig. 9).

Discussion

DR is an important substantial microvascular impedi-
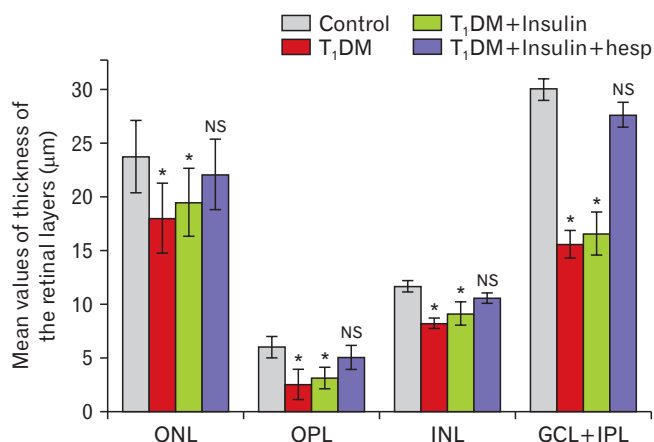
Fig. 7. Statistical analysis of thickness of the retinal layers (µm) in different studied groups. Values are presented as mean±SD. Significant with control (*P<0.05). ONL, outer nuclear layer; OPL, outer plexiform layer; INL, inner nuclear layer; GCL, ganglion cell layer; IPL, inner plexiform layer; T₁DM, type 1 diabetes mellitus; hesp, hesperetin 7-rhamnoglucoside; NS, non-significant with control.
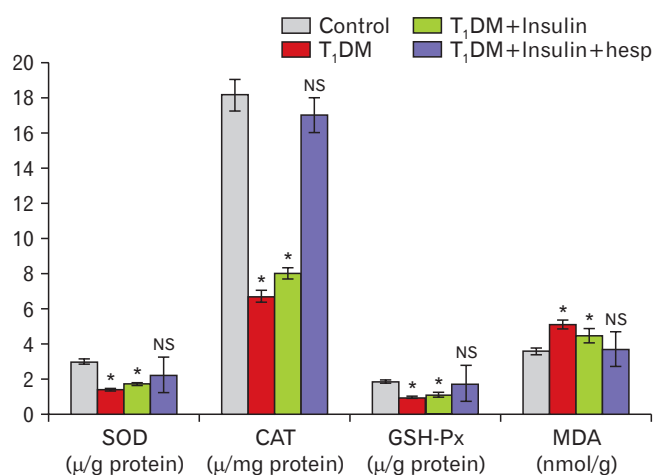
Fig. 8. Statistical analysis of retinal content of antioxidant enzymes SOD, CAT, GSH-Px, and oxidant marker MDA in all studied groups. Values are presented as mean±SD. Significant with control (*P<0.05). SOD, superoxide dismutase; CAT, catalase; GSH-Px, glutathione peroxidase; MDA, malondialdehyde; NS, non-significant with control; T₁DM, type 1 diabetes mellitus; hesp, hesperetin 7-rhamnoglucoside.

Fig. 9. Statistical analysis of relative gene expression of GFAP and VEGF in rat retina in different studied groups. Significant with control (***P≤0.001). VEGF, vascular endothelial growth factor; GFAP, glial fibrillary acidic protein; T₁DM, type 1 diabetes mellitus; hesp, hesperetin 7-rhamnoglucoside; NS, non-significant with control.

used agent in animal models to induce biochemical and pathological changes simulating the onset of DR arising in humans [26].

Regarding positive control rats, hesp administration has no influence on retinal histological structure and biochemical markers (data were not shown). This finding conforms to the findings of Ali et al. [27]. Group II (T₁DM) in this study exhibited several histological and ultrastructural retinal changes associated with hyperglycemia. Similar results were reported in published studies [28, 29]. Roy et al. [30] have clarified that DR is accompanied by mitochondrial dysfunction and endoplasmic reticulum stress. This study revealed a significant decrease in the thickness of different retinal layers compared with that in the control group. Such findings have been confirmed by morphometric analysis and conform to previous reports, which concluded increased apoptotic retinal neurons in rats with diabetes. The neuronal pathology of diabetic retinal changes is a sequence of oxidative stress [31]. In contrast, Toyoda et al. [32] have reported that long-term hyperglycemia causes retinal thickening due to the escape of blood constituents from retinal vessels.

Our biochemical results have shown an increase in oxidative levels and a decline in antioxidant enzymes. The imbalance between both oxidants and antioxidants is a significant cause of the initiation and progression of DR [33]. The retina is more susceptible to develop oxidative stress due to its high oxygen demands, the large amounts of polyunsaturated fatty acids in its structure, and the natural continuous light exposure [34].

ment of diabetes mellitus. All patients with diabetes are at risk of retinopathy; however, patients with T₁DM are at a higher risk [25].

This study was designed to assess the probable ameliorative influence of hesp along with insulin compared with that of insulin alone on diabetic retinal changes in rats with T₁DM.

STZ was used in this study as it is the most commonly

This study revealed a significant increase in *GFAP* gene expression in group II, which was supported by the findings of previous studies [30, 35]. Hyperglycemia leads to the activation of Müller cells and subsequent gliosis so that GFAP overexpression can be measured as a retinal injury marker [36]. Some authors have correlated these changes to deficient neurotropic factors in DR, which could stop the degeneration of retinal photoreceptor cells and promote the axonal regeneration of ganglion cells [37].

The current results showed a significant increase in the level of VEGF in group II compared with that in the control group. VEGF is a proangiogenic factor regulator that damages the blood-retina barrier (BRB) by several mechanisms, leading to increased vascular permeability and the development of retinal edema. An imbalance between proangiogenic mediators and ischemia result in the growth of abnormal leaky blood vessels, eventually leading to retinal neovascularization [3, 38].

This study showed a significant rise in AGEs in group II. These results conform to those of Yamagishi et al. [39]. AGEs provoke pathogenic mechanisms, including diminished endothelial nitric oxide synthase (eNOS) activities, pericyte death, decreased nerve growth factor (NGF) and elevated expression of GFAP [40].

Examination of the retina of group III showed little improvement in ultrastructure and biochemical results. Furthermore, many neuronal alterations were found. These findings are inconsistent with those reported by Kuo et al. [41].

Group IV showed an almost normal retinal histological and ultrastructural picture with improvements in the biochemical results. This conforms to the findings of Xin et al. [42], who suggested that hesp plays a key role in inhibiting apoptosis in the retinae by decreasing both caspase-9 and caspase-3. Hesp has a stronger antioxidant activity than other flavanones [43]. Recent studies have shown that hesp could normalize hyperglycemia in rat models with STZ-induced diabetes by changing the action of glucose-moderating enzymes and decreasing lipid levels in both the serum and liver [11]. Furthermore, Liu et al. [44] have reported that hesp regains mitochondrial function by preventing the dissipation of membrane potential in the mitochondria and enhances the secretion of cytochrome c into cytosol. The therapeutic actions of hesp in the rescue of retinal neuro-inflammation, oxidative stress, apoptosis, and edema have been clearly shown in the studies by Kumar et al. [45]. They have concluded that hesp can be useful for preventing neuro-vascular problems, such as DR. Moreover, hespsignificantly suppressed BRB damage in cases of DR [46]. Furthermore, hesp was suggested to increase ocular blood circulation, which leads to retinal function improvement through nitric oxide (NO) bioavailability enhancement [47].

In contrast, nitric oxide synthase-2 (NOS-2) was suggested to be the result of cell death by increasing oxidative stress via caspase activation and mitochondrial dysfunction [48].

Furthermore, this study revealed a significant decrease in AGE-positive immunoreactivity in all retinal layers in group IV. It has been suggested that hesp decreases the formation of AGE *in vitro* in animal trials [49]. Furthermore, it significantly decreases HbA1c levels, thus permitting its neuroprotective action [50]. The retina has a highly potent antioxidant defense system, including free radical scavengers, such as α-tocopherol, GSH, ascorbic acid, and antioxidant enzymes, such as GSH-Px, SOD, and CAT [51]. The rats with diabetes in this study showed reduced GSH levels and decreased activity of SOD and CAT compared with healthy rats. These variations in antioxidant parameters agree with previous studies [52, 53]. Hesp-treated retinae showed recovery of the antioxidant defense system to normal levels and the prohibition of retinal inflammatory transformations. Hesp being a flavanone provides a potent antioxidant action, which moderates the enzymatic activity efficiently [54, 55]. Similarly, in this study, a positive inflection of GSH and antioxidant enzymes was detected. Moreover, this study demonstrated the therapeutic qualifications of hesp in rescuing retinal oxidation and apoptosis as a result of uncontrolled diabetes mellitus.

In conclusion, it can be assumed that dietary flavonoids, such as hesp, can be combined with insulin for effectively inhibiting diabetes-associated neurovascular impediments, such as DR. Moreover, it supports the potential of hesp to inhibit receptor of AGEs (RAGE)-mediated cellular cascades causing improved retinal changes, including angiogenesis, hypoxia, and cellular apoptosis, in animal models with STZ-induced diabetes.

ORCID

Azza Saad Shehata:
https://orcid.org/0000-0002-5095-107X
Dalia Abduelmoein Mohamed:
https://orcid.org/0000-0003-0471-4687

Sherein Mahmoud Hagras:
https://orcid.org/0000-0001-6560-3839
Shimaa Mohsen El-Beah:
https://orcid.org/0000-0003-1398-0194
Heba Mohamed Elnegris:
https://orcid.org/0000-0002-6265-6959

Author Contributions

Conceptualization: ASS, DAM, HME. Data acquisition: DAM, HME. Data analysis or interpretation: SMH, SME, HME. Drafting of the manuscript: DAM, HME. Critical revision of the manuscript: ASS, SME, HME. Approval of the final version of the manuscript: all authors.

Conflicts of Interest

No potential conflict of interest relevant to this article was reported.

Acknowledgements

References

1. Mwangi MW, Githinji GG, Githinji FW. Knowledge and awareness of diabetic retinopathy amongst diabetic patients in Kenyatta National Hospital, Kenya. Int J Hum Soc Sci 2011;1:140-6.

2. Tarr JM, Kaul K, Chopra M, Kohner EM, Chibber R. Pathophysiology of diabetic retinopathy. ISRN Ophthalmol 2013;2013:343560.

3. Altmann C, Schmidt MHH. The role of microglia in diabetic retinopathy: inflammation, microvasculature defects and neurodegeneration. Int J Mol Sci 2018;19:110.

4. Grosso A, Cheung N, Veglio F, Wong TY. Similarities and differences in early retinal phenotypes in hypertension and diabetes. J Hypertens 2011;29:1667-75.

5. Sasongko MB, Wong TY, Nguyen TT, Kawasaki R, Jenkins A, Shaw J, Wang JJ. Serum apolipoprotein AI and B are stronger biomarkers of diabetic retinopathy than traditional lipids. Diabetes Care 2011;34:474-9.

6. Kowluru RA, Chan PS. Oxidative stress and diabetic retinopathy. Exp Diabetes Res 2007;2007:43603.

7. Tahrani AA, Piya MK, Kennedy A, Barnett AH. Glycaemic control in type 2 diabetes: targets and new therapies. Pharmacol Ther 2010;125:328-61.

8. Li WQ, Park Y, Wu JW, Ren JS, Goldstein AM, Taylor PR, Hollenbeck AR, Freedman ND, Abnet CC. Index-based dietary patterns and risk of esophageal and gastric cancer in a large cohort study. Clin Gastroenterol Hepatol 2013;11:1130-6.e2.

9. Yari Z, Movahedian M, Imani H, Alavian SM, Hedayati M, Hekmatdoost A. The effect of hesperidin supplementation on metabolic profiles in patients with metabolic syndrome: a randomized, double-blind, placebo-controlled clinical trial. Eur J Nutr 2020;59:2569-77.

10. Kawaguchi K, Mizuno T, Aida K, Uchino K. Hesperidin as an inhibitor of lipases from porcine pancreas and Pseudomonas. Biosci Biotechnol Biochem 1997;61:102-4.

11. Akiyama S, Katsumata S, Suzuki K, Ishimi Y, Wu J, Uehara M. Dietary hesperidin exerts hypoglycemic and hypolipidemic effects in streptozotocin-induced marginal type 1 diabetic rats. J Clin Biochem Nutr 2010;46:87-92.

12. Kandhare AD, Mukherjee A, Bodhankar SL. Effect of hesperidin in bleomycin-induced pulmonary fibrosis in rats: critical role of NRF-2, TNF-A, and IL-1B. Value Health 2017;20:A887-8.

13. National Research Council (U.S.), Institute of Laboratory Animal Resources. Guide for the care and use of laboratory animals. Washington, D.C.: National Academy Press; 1996. p. 21-55.

14. Kohzaki K, Vingrys AJ, Bui BV. Early inner retinal dysfunction in streptozotocin-induced diabetic rats. Invest Ophthalmol Vis Sci 2008;49:3595-604.

15. Subramanian P, Anandan R, Jayapalan JJ, Hashim OH. Hesperidin protects gentamicin-induced nephrotoxicity via Nrf2/HO-1 signaling and inhibits inflammation mediated by NF-κB in rats. J Funct Foods 2015;13:89-99.

16. Foureaux G, Nogueira BS, Coutinho DC, Raizada MK, Nogueira JC, Ferreira AJ. Activation of endogenous angiotensin converting enzyme 2 prevents early injuries induced by hyperglycemia in rat retina. Braz J Med Biol Res 2015;48:1109-14.

17. Fröde TS, Medeiros YS. Animal models to test drugs with potential antidiabetic activity. J Ethnopharmacol 2008;115:173-83.

18. Bancroft JD, Gamble M. Theory and practice of histological techniques. 5th ed. London: Churchill Livingstone; 2002.

19. Kiernan JA. Histological and histochemical methods: theory and practice. 3rd ed. Oxford: Butterworth Heinemann; 2000.

20. Kim J, Kim CS, Lee YM, Sohn E, Jo K, Kim JS. Litsea japonica extract inhibits neuronal apoptosis and the accumulation of advanced glycation end products in the diabetic mouse retina. Mol Med Rep 2015;12:1075-81.

21. Glauert AM, Lewis PR. Biological specimen preparation for transmission electron microscopy. London: Portland Press; 1998.

22. Woo TT, Li SY, Lai WW, Wong D, Lo AC. Neuroprotective effects of lutein in a rat model of retinal detachment. Graefes Arch Clin Exp Ophthalmol 2013;251:41-51.

23. Saenz-de-Viteri M, Heras-Mulero H, Fernández-Robredo P, Recalde S, Hernández M, Reiter N, Moreno-Orduña M, García-

Layana A. Oxidative stress and histological changes in a model of retinal phototoxicity in rabbits. Oxid Med Cell Longev 2014;2014:637137.

24. Livak KJ, Schmittgen TD. Analysis of relative gene expression data using real-time quantitative PCR and the 2(-Delta Delta C(T)) method. Methods 2001;25:402-8.

25. Kashim RM, Newton P, Ojo O. Diabetic retinopathy screening: a systematic review on patients' non-attendance. Int J Environ Res Public Health 2018;15:157.

26. Jiang T, Chang Q, Cai J, Fan J, Zhang X, Xu G. Protective effects of melatonin on retinal inflammation and oxidative stress in experimental diabetic retinopathy. Oxid Med Cell Longev 2016;2016:3528274.

27. Ali AM, Gabbar MA, Abdel-Twab SM, Fahmy EM, Ebaid H, Alhazza IM, Ahmed OM. Antidiabetic potency, antioxidant effects, and mode of actions of *Citrus reticulata* fruit peel hydroethanolic extract, hesperidin, and quercetin in nicotinamide/streptozotocin-induced Wistar diabetic rats. Oxid Med Cell Longev 2020;2020:1730492.

28. Saxena Y, Purwar B, Meena H, Sarthi P. Dolichos biflorus Linn. ameliorates diabetic complications in streptozotocin induced diabetic rats. Ayu 2014;35:442-6.

29. Yang QH, Zhang Y, Jiang J, Wu MM, Han Q, Bo QY, Yu GW, Ru YS, Liu X, Huang M, Wang L, Zhang XM, Fang JM, Li XR. Protective effects of a novel drug RC28-E blocking both VEGF and FGF2 on early diabetic rat retina. Int J Ophthalmol 2018;11:935-44.

30. Roy S, Trudeau K, Roy S, Tien T, Barrette KF. Mitochondrial dysfunction and endoplasmic reticulum stress in diabetic retinopathy: mechanistic insights into high glucose-induced retinal cell death. Curr Clin Pharmacol 2013;8:278-84.

31. Ozdemir G, Ergün Y, Bakariş S, Kılınç M, Durdu H, Ganiyusufoğlu E. Melatonin prevents retinal oxidative stress and vascular changes in diabetic rats. Eye (Lond) 2014;28:1020-7.

32. Toyoda F, Tanaka Y, Shimmura M, Kinoshita N, Takano H, Kakehashi A. Diabetic retinal and choroidal edema in SDT rats. J Diabetes Res 2016;2016:2345141.

33. Soufi FG, Mohammad-Nejad D, Ahmadieh H. Resveratrol improves diabetic retinopathy possibly through oxidative stress - nuclear factor κB - apoptosis pathway. Pharmacol Rep 2012;64:1505-14.

34. Qian H, Ripps H. Neurovascular interaction and the pathophysiology of diabetic retinopathy. Exp Diabetes Res 2011;2011:693426.

35. Krady JK, Basu A, Allen CM, Xu Y, LaNoue KF, Gardner TW, Levison SW. Minocycline reduces proinflammatory cytokine expression, microglial activation, and caspase-3 activation in a rodent model of diabetic retinopathy. Diabetes 2005;54:1559-65.

36. Çerman E, Akkoç T, Eraslan M, Şahin Ö, Özkara S, Vardar Aker F, Subaşı C, Karaöz E, Akkoç T. Retinal electrophysiological effects of intravitreal bone marrow derived mesenchymal stem cells in streptozotocin induced diabetic rats. PLoS One 2016;11:e0156495.

37. Liang X, Zhou H, Ding Y, Li J, Yang C, Luo Y, Li S, Sun G, Liao X, Min W. TMP prevents retinal neovascularization and imparts neuroprotection in an oxygen-induced retinopathy model. Invest Ophthalmol Vis Sci 2012;53:2157-69.

38. Chen W, Yao X, Zhou C, Zhang Z, Gui G, Lin B. Danhong Huayu Koufuye prevents diabetic retinopathy in streptozotocin-induced diabetic rats via antioxidation and anti-inflammation. Mediators Inflamm 2017;2017:3059763.

39. Yamagishi S, Inagaki Y, Amano S, Okamoto T, Takeuchi M, Makita Z. Pigment epithelium-derived factor protects cultured retinal pericytes from advanced glycation end product-induced injury through its antioxidative properties. Biochem Biophys Res Commun 2002;296:877-82.

40. Raghu G, Akileshwari C, Reddy VS, Reddy GB. Attenuation of diabetic retinopathy in rats by ellagic acid through inhibition of AGE formation. J Food Sci Technol 2017;54:2411-21.

41. Kuo JZ, Wong TY, Rotter JI. Challenges in elucidating the genetics of diabetic retinopathy. JAMA Ophthalmol 2014;132:96-107.

42. Xin X, Li Y, Liu H. Hesperidin ameliorates hypobaric hypoxia-induced retinal impairment through activation of Nrf2/HO-1 pathway and inhibition of apoptosis. Sci Rep 2020;10:19426.

43. Maekawa S, Sato K, Fujita K, Daigaku R, Tawarayama H, Murayama N, Moritoh S, Yabana T, Shiga Y, Omodaka K, Maruyama K, Nishiguchi KM, Nakazawa T. The neuroprotective effect of hesperidin in NMDA-induced retinal injury acts by suppressing oxidative stress and excessive calpain activation. Sci Rep 2017;7:6885.

44. Liu WY, Liou SS, Hong TY, Liu IM. Protective effects of hesperidin (citrus flavonone) on high glucose induced oxidative stress and apoptosis in a cellular model for diabetic retinopathy. Nutrients 2017;9:1312.

45. Kumar B, Gupta SK, Srinivasan BP, Nag TC, Srivastava S, Saxena R, Jha KA. Hesperetin rescues retinal oxidative stress, neuroinflammation and apoptosis in diabetic rats. Microvasc Res 2013;87:65-74.

46. Shi X, Liao S, Mi H, Guo C, Qi D, Li F, Zhang C, Yang Z. Hesperidin prevents retinal and plasma abnormalities in streptozotocin-induced diabetic rats. Molecules 2012;17:12868-81.

47. Kara S, Gencer B, Karaca T, Tufan HA, Arikan S, Ersan I, Karaboga I, Hanci V. Protective effect of hesperetin and naringenin against apoptosis in ischemia/reperfusion-induced retinal injury in rats. ScientificWorldJournal 2014;2014:797824.

48. Eltony SA, Mohaseb HS, Sayed MM, Ahmed AA. Metformin treatment confers protection of the optic nerve following photoreceptor degeneration. Anat Cell Biol 2021;54:249-58.

49. Visnagri A, Kandhare AD, Chakravarty S, Ghosh P, Bodhankar SL. Hesperidin, a flavanoglycone attenuates experimental diabetic neuropathy via modulation of cellular and biochemical marker to improve nerve functions. Pharm Biol 2014;52:814-28.

50. Kakadiya J, Patel D, Shah N. Effect of hesperidin on renal complication in experimentally induced renal damage in diabetic

Sprague dawley rats. J Ecobiotechnol 2010;2:45-50.

51. Kowluru RA, Tang J, Kern TS. Abnormalities of retinal metabolism in diabetes and experimental galactosemia. VII. Effect of long-term administration of antioxidants on the development of retinopathy. Diabetes 2001;50:1938-42.

52. Obrosova IG, Drel VR, Kumagai AK, Szábo C, Pacher P, Stevens MJ. Early diabetes-induced biochemical changes in the retina: comparison of rat and mouse models. Diabetologia 2006;49:2525-33.

53. Gupta SK, Kumar B, Nag TC, Agrawal SS, Agrawal R, Agrawal P, Saxena R, Srivastava S. Curcumin prevents experimental diabetic retinopathy in rats through its hypoglycemic, antioxidant, and anti-inflammatory mechanisms. J Ocul Pharmacol Ther 2011;27:123-30.

54. Aranganathan S, Selvam JP, Sangeetha N, Nalini N. Modulatory efficacy of hesperetin (citrus flavanone) on xenobiotic-metabolizing enzymes during 1,2-dimethylhydrazine-induced colon carcinogenesis. Chem Biol Interact 2009;180:254-61.

55. Aranganathan S, Nalini N. Efficacy of the potential chemopreventive agent, hesperetin (citrus flavanone), on 1,2-dimethylhydrazine induced colon carcinogenesis. Food Chem Toxicol 2009;47:2594-600.